Received 6 April 2021; revised 3 June 2021; accepted 5 June 2021.
Date of publication 8 June 2021; date of current version 15 June 2021.

Digital Object Identifier 10.1109/OAJPE.2021.3087547

Reliability Assessment of Converter-Dominated Power Systems Using Variance-Based Global Sensitivity Analysis

BOWEN ZHANG (Graduate Student Member, IEEE), MENGQI WANG (Senior Member, IEEE), AND WENCONG SU (Senior Member, IEEE)

Department of Electrical and Computer Engineering, University of Michigan-Dearborn, Dearborn, MI 48128 USA
CORRESPONDING AUTHORS: W. SU (wencong@umich.edu) AND M. WANG (mengqiw@umich.edu)

ABSTRACT With the proliferation of renewable energy and power electronic converters in power systems, the reliability issue has raised more research attention than ever before. This paper proposes a comprehensive framework to assess the reliability of a power system considering the effect from various power converter uncertainties. For the converter stage, we formulate a reliability model for each power converter based on several semiconductor devices, for which ambient uncertainties and converter topologies are considered. For the system stage, we estimate system reliability indicators through a non-sequential Monte Carlo simulation and calculate their variances. Afterward, we leverage machine learning regression algorithms between two stages to establish a nonlinear reliability relation. Moreover, a variance-based sensitivity analysis (SA) is conducted to rank and identify the most influential converter uncertainties with respect to the variance of system EENS. Based on the SA conclusions, system operators can take proactive actions to mitigate the potential risk of the system.

INDEX TERMS Power system reliability, power converters, machine learning, power electronics, sensitivity analysis.

I. INTRODUCTION

THE incorporation of renewable energy resources (RES) in power systems has brought several challenges to realizing a reliable power delivery. That said, the proliferation of RES has been significantly accompanied by the penetration of various power electronic converters. Notably, the power electronic converter plays a fundamental role during energy conversion [1]. Consequently, from a reliability point of view, the system has become more complicated compared with a traditional system.

A power system's reliability is defined as a measurement of its ability to cope with customer demands. Many existing research works investigated the reliability issue of conventional power systems [2]. The reliability of power systems with RESs such as wind turbines (WTs) or solar photovoltaics (PVs) is investigated in [3], [4]. The authors in [5] and [6] conducted a system reliability assessment considering diverse load demands in a large-scale WT system or PV system. However, failures caused by power electronic converters connected to those RESs have not raised much attention in most published research works. According to field data and industrial experiences, power converters are one of the frequent sources of failure in many electrical applications [7].

From a power electronics perspective, many researchers devoted their research focus on assessing various converters' reliability from both device and overall converter layer. The reliability of a power converter is largely determined by the performance of critical components. In [8], efficiency and cost functions of a DC-DC boost converter integrated with solar panels were evaluated. Authors in [7] performed a reliability estimation for critical devices of a WT converter where the thermal loading of each device was considered. For those deregulated systems, transmission and generation may be operated by various entities and renewable energies can

be directly delivered to local users. However, for traditional regulated power systems, effective RES power conversion can secure only that all available renewable energies are injected into the main power system. Whether these power inputs can be successfully transferred and satisfy the load demand in future power systems is still questionable.

Based on these surveys from both the power system and power electronics fields, we can conclude that more uncertainty and complexity are introduced in today's power systems compared with traditional systems. The output power of each RES is determined by several ambient variables which are predictable but uncontrollable. Moreover, power conversion interfaces, typically represented by one or more power converters, become an essential bridge between each RES and the main grid. However, there were that few papers bridged the gap between system uncertainty and converter reliability. A DC-DC converter reliability model was formulated in [8] in evaluating the reliability of an energy storage system. Still, the paper did not investigate the reliability impact of different converter types on the overall system. The authors in [1] incorporated various converter reliability models into system reliability analysis but did not investigate the system reliability under transmission level. Thus, it is necessary to intensify the importance of power electronic converters and investigate their potential effects when assessing the reliability of a power system under the proliferation of RESs and power electronic interfaces [9].

Meanwhile, various uncertain parameters are introduced in power systems due to intermittent RESs and the operational structure. These uncertainties may have significant influence on the system's reliability performance. The authors in [10] highlighted that a conservative power system assessment or non-optimal maintenance solutions would be made by decision-makers if spatiotemporal uncertain parameters are neglected. In [11], the authors implemented several numerical sensitivity analysis (SA) methods to investigate the most important uncertainty affecting the reliability of power systems. Therefore, implementing an appropriate SA on the proposed reliability framework is essential in order to interpret the system reliability behavior and identify the effects that emerging power converters will have on system reliability. Identifying the most critical uncertainties, i.e., the most influential pair of an RES and its connected power converter on the system reliability will help system operators and stakeholders to better arrange the maintenance schedule and facilitate better system operation.

SA is mainly categorized into two classes: local SA (LSA) and global SA (GSA). GSA has a variety of applications in power systems, such as reconfiguring power networks [12], allocating voltage control devices [13], and improving transmission capacity [14]. However, most conventional GSAs neglect the uncertain parameters from RESs and power converters and may not provide accurate results in terms of system reliability characteristics. In the last decade, a variety of implementations of the variance-based GSA have been presented, which indicates that the variance is a universal

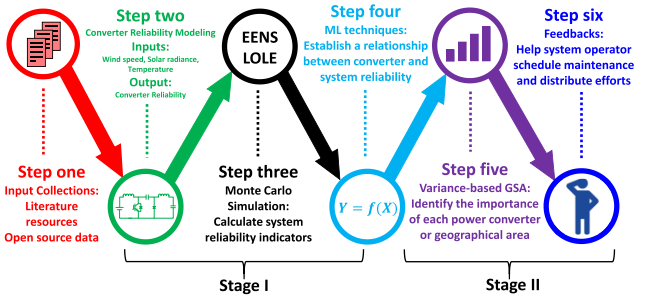

FIGURE 1. Six steps of the proposed two-stage reliability assessment framework.

and proper index to depict the output variability. Another advantage of variance-based GSA over other GSA methods is that system variance has been validated as a proper index to quantify the contribution of each input uncertainty without any hypothesis on the linearity or monotonicity of the model [15].

In this paper, the first stage of the framework utilizes a group of failure rates for various power electronic devices and formulates converters' reliability. The second stage of the proposed framework presents for the first time the application of the variance-based GSA to identify the contribution of each converter uncertainty to the variance of the system reliability indicator. This novel application is of critical importance as future power systems become increasingly implemented with RESs and power converters. The research purpose of this stage is to provide instructive information to system operators, achieve better system operation planning, and promote the application of more advanced SA methods in power systems.

Fig. 1 generalizes each step of the proposed reliability assessment framework. In the first step, we collect ambient conditions from available literature and open-source data. Each converter reliability is then formulated based on physical/thermal dynamics of several power electronic devices and converter topology. In step three, system reliability indicators such as expected energy not served (EENS) and loss of load expectation (LOLE) are calculated through a set of Monte Carlo simulations. Further, in step four, we establish a relationship between the converter and the system stage from the reliability perspective by utilizing machine learning (ML) regression techniques to capture the converter dependence structure for several components and calculate the reliability indicators of a converter-penetrated system at scale.

According to the aforementioned reliability and uncertainty issues posed by the proliferation of RESs and power electronic converters in future power systems, this paper has the following contributions:

1) The proposed reliability assessment of a power system consists of two stages. In the first stage, we collect hourly based ambient data to formulate the failure model for each semiconductor device. Both physical and thermal characteristic parameters of each device are estimated to achieve the device failure rate in an accurate manner.

2) The scale of system complexity and uncertainty will increase as more RESs and converters are implemented into the power system. How the performance of each converter would affect the system-level reliability is yet to be investigated. Therefore, this paper leverages ML regression algorithms to establish a reliability relation between converter and system reliability. We provide a fundamental guideline of evaluating complex power system reliability from power converter perspective. The established nonlinear relation maintains the flexibility of adding new converter into consideration such that comprehensive reliability information from both converter and system level can be revealed to system operators.

3) The uncertainty parameters coming from power converters are yet to be considered when conducting traditional GSA. In the second stage, the variance-based GSA method is applied to the proposed power system to provide instructive information to system operators and stakeholders such that better operational planning can be achieved. This novel application is also intended to promote the development of the implementation of more advanced SA methods in power systems such that interested researchers can further interpret the reliability behavior of future power systems.

The rest of this paper is organized as follows. First, the formulation of power converter reliability is presented in Section II. Section III presents basic information of ML and multiple regression algorithms. Section IV introduces the fundamental procedure of how the variance-based GSA is integrated into the power system. The Monte Carlo simulation and the system overview are presented in Section V. The proposed reliability framework is verified on the IEEE 24-bus RTS in Section VI. Conclusions and future works are summarized in Section VII.

II. FORMULATION FOR CONVERTER RELIABILITY

This section introduces the reliability quantification of each power electronic converter. As shown in equation (1), converter reliability $R(t)$ is estimated, where λ denotes the overall failure rate. λ is time-invariant and is conventionally treated as a constant value [7].

$$R(t) = e^{-\lambda t} \tag{1}$$

However, λ is affected by various uncertainties, including the type of integrated device, thermal loading and environmental parameters. To consider these factors, we collect hourly based ambient data and assume each uncertainty follows a pre-defined probability distribution over a 1-year time span such that in each converter, the values of λ and $R(t)$ are determined in a more accurate manner. The following subsections A and B present the reliability model of WT and PV converter, respectively. The detailed formulation can be referred to in [9].

A. WT CONVERTER MODELING

We consider a typical WT system, with the detailed schematic being presented in Appendix B. The WT output power $P_{wt,t}$ at time t can be estimated by the wind speed v_t [3]. We collect hour-based wind speed such that $P_{wt,t}$ at hour t, is calculated by equation (2), where P_{rated} denotes the rated capacity; v_{ci}, v_{co}, and v_r refer to the cut-in, cut-out, and rated wind speeds, respectively [26].

$$P_{wt,t} = \begin{cases} 0, & 0 \le v_t \le v_{ci} \\ \left(A + Bv_t + CV_t^2\right) P_{rated}, & v_{ci} \le v_t \le v_r \\ P_{rated}, & v_r \le v_t \le v_{co} \\ 0, & v_t \ge v_{co} \end{cases} \tag{2}$$

The WT output power will, consequently, determine the power losses of each integrated device. However, monitoring/measuring all devices will be inefficient and redundant. Therefore, we identify critical devices and then, estimate their power losses. Critical devices identified in this WT system are mainly diodes and IGBTs. Their total power losses are the sum of switching loss and conduction loss. Both losses are calculated through various electrical parameters such as voltage drops, resistance, and the switching frequency [1].

$$P_{loss\_IGBT} = P_{IGBT\_cd} + P_{IGBT\_sw} \tag{3}$$

$$P_{loss\_diode} = P_{diode\_cd} + P_{diode\_sw} \tag{4}$$

As shown in (3) and (4), the power loss of a diode/IGBT is calculated. The subscript *cd* denotes the conduction loss while *sw* refers to the switching loss. Detailed equations for calculating $P_{IGBT\_cd}, P_{IGBT\_sw}, P_{diode\_cd}$ and P_{diode_sw} are provided in Appendix C.

Both the generation-side inverter and the grid-side inverter are considered in this WT system. Their topologies are assumed as known such that the number of diodes/IGBTs are determined. We assume that all components are connected in series from a reliability point of view since one failed component will likely bring a failure of entire converter. The total power losses denoted by $P_{WT\_conv\_loss}$ is estimated in (5), where n_D and n_G refers to the number of diodes and IGBTs, respectively.

$$P_{WT\_conv\_loss} = \sum_{n=1}^{n_D} P_{loss\_IGBT} + \sum_{n=1}^{n_G} P_{loss\_diode} \tag{5}$$

One of the critical factors which has an impact on the device failure rate is its thermal dynamics. We apply the calculated total power losses and ambient temperature data to estimate device thermal parameters including diode/IGBT junction temperature, thermal stress factor, thermal resistance and the temperature cycling factor. Their detailed calculations are provided in Appendix C. Afterward, we derive the device failure rate model by collecting all calculation results from above. The FIDES approach [27] which is considered as the latest update on failure rate prediction for power electronic components, is applied, and the failure rate model of a diode/IGBT is presented in (6):

$$\lambda_{j,t} = \sum_{i}^{N_s} (\lambda_{0Th}\pi_{Tj,t} + \lambda_{0TC}\pi_{TCj,t})\pi_{In}\pi_{Pm}\pi_{Pr} \tag{6}$$

where $\lambda_{j,t}$ is the failure rate of device j at hour t, N_s is the number of device operating states; λ_{0Th} and λ_{0TC} refer to fundamental failure elements of a device, respectively; $\pi_{Tj,t}$ and $\pi_{TCj,t}$ represent thermal stress and temperature cycling parameter of device j at hour t, respectively; π_{ln} is considered as the contribution of overstress which is estimated by the device sensitivity coefficient to overstress and the device application area; π_{Pm} is the device quality factor; and π_{Pr} reflects the aging effect of the device life cycle.

$$R_{WT_{conv}}(t) = e^{-(\sum_{j=1}^{N_j} \lambda_{j,t})t} \tag{7}$$

Thus, the overall WT converter failure rate is derived, and its reliability is calculated by (7), where N_j is the number of all devices considered above.

B. PV CONVERTERS MODELING

We consider a typical PV system consisting of a PV array, a DC-DC boost converter, and a DC-AC inverter. The detailed schematic of the PV system is provided in Appendix B.

Similarly, the first step is to determine the PV output power. Ambient temperature, as well as solar radiance are considered as the inputs. We assume a maximum power point tracking mechanism (MPPT) in terms of the power generated by PV panels. As shown in equation (8), $P_{pv,t}$ stands for the power produced by PV panels at hour t, SR_t represents the intensity of solar radiation, S_0 refers to the maximum solar radiance, P_{max} stands for the maximum power generated under standard conditions, γ refers to the temperature coefficient, T_t represents the ambient temperature at hour t, and T_0 is the standard temperature [17].

$$P_{pv,t} = \frac{SR_t}{S_0} P_{max}[1 + \gamma_0(T_t - T_0)] \tag{8}$$

The power losses and the thermal effects of major semiconductor devices are considered, and they are calculated through the same procedure from (3) to (6). Afterward, the PV converter reliability is calculated by (9), where N_m is the number of devices implemented, and $\lambda_{m,t}$ refers to the failure rate of device m at hour t. Detailed calculations are also provided in Appendix C.

$$R_{PV_{conv}}(t) = e^{-(\sum_{j=1}^{N_m} \lambda_{m,t})t} \tag{9}$$

III. RELIABILITY MAPPING THROUGH ML TECHNIQUES

In the proposed framework, ML regression algorithms are leveraged to conduct a reliability mapping between converter and system stage for the following reasons. First, to investigate the potential impact on system reliability due to power converter failures/outages, the reliability relation between various power converters and overall system is worth establishing; however, as more RESs and converters are integrated into the power system, the system uncertainty and complexity continue to increase, which intensifies this kind of relation become nonlinear. Consequently, it is unlikely to express this reliability relation with an analytical manner. However, ML algorithms are capable of dealing with nonlinear relation. One of the impressive characteristics of ML is its outstanding ability to explore the relation between various input and output data with arbitrary accuracy [18]. Second, this relation may need several updates as RES, converter integrations and also system structure will be further enhanced in the future. ML techniques maintain the flexibility for embedding new parameters as additional input features such that the nonlinear relation can be generalized without losing much computational cost. We introduce the fundamental concepts of ML regression and the proposed two-stage reliability mapping formulation in this section.

A. CONCEPTS

The reliability mapping between converter and system level data can be statistically modeled as a typical regression problem. We describe the logic of the regression algorithm as follows: In the training data, assume there exists n pairs under a set $\{(x_k, y_k), k = 1, 2, \ldots, n\}$. x_k represents the vector of input feature k and y_k is the system output vector. x_k consists of a data array where a sample data point is targeted by all other data [18]. During each testing iteration, the value of this sample point is arbitrarily predicted from x_k, and is further compared accordingly with its actual value in y_k (y_k is continuous). A data mapping refers to an effective function between x and y such that each y_k value can be predicted with limited error when x_k is given, even if the established function is nonlinear. In the proposed framework, we consider reliability data of all converters as the mapping input features while continuous system reliability indicators such as EENS and LOLE are assumed as output labels. Two ML regression algorithms, namely, support vector regression (SVR) and random forests (RF) are applied to realize the reliability mapping. It is worth noting that other ML regression algorithms may have comparable performance. However, the main purpose of this paper is not to optimize the regression model, but to explore a potential nonlinear relation between converter and system reliability data by leveraging ML regression algorithms.

B. SUPPORT VECTOR REGRESSION

SVR has been applied to establish a data mapping or a function estimator, as shown in (10), by utilizing a subset of the provided dataset [19]. It can provide a sparse pattern of solutions and maintain flexible on the model complexity. In SVR, different kernel functions are commonly applied to map the input space, e.g., n power converters, into a higher dimensional feature space, which introduces non-linearity in solutions and to conduct a linear regression in the feature space. The SVR model is formulated by the following function:

$$Y = f(x) = W \cdot \phi(X) + b \tag{10}$$

where Y represents the set of system reliability indicator values, W is a weighted feature vector, $\phi(\cdot)$ represents the mapping and b refers to the predicted constant coefficient. The function f should be flat to avoid over-fitting and loosely

fit the training data. The detailed SVR formulation can be found in [19].

C. RANDOM FORESTS

An RF model is a ML algorithm for dealing with classification or regression problems [20]. An ensemble of decision trees is constructed from the training data set and the mean value of all trees is applied to predict the value for new input data. Specifically, consider a variable of interest Y and a set of input variables X. $\hat{f}$ denotes the predicting function. Let $L_n = \{(X_1, Y_1), \ldots, (X_n, Y_n)\}$ be a learning set. Since the actual prediction error is unknown, we estimate the error R based on observing a validation sample $\bar{D}$, as shown in (11). The growing procedure of each tree can be found in [20].

$$R(\hat{f}, \bar{D}) = \frac{1}{|\bar{D}|} \sum_{(X_i, Y_i) \in \bar{D}} \left(Y_i - \hat{f}(X_i)\right)^2 \tag{11}$$

$$RMSE = \sqrt{\frac{1}{n} \sum_{k=1}^{n} \left(y_k - \hat{y}_k\right)^2} \tag{12}$$

$$R_{-squared} = 1 - \frac{\sum_{k=1}^{n} \left(y_k - \hat{y}_k\right)^2}{\sum_{k=1}^{n} \left(y_k - \bar{y}_k\right)^2} \tag{13}$$

The general steps of the proposed mapping procedure are presented in Algorithm 1. Equation (12) and (13) apply two statistical measurements, namely, root mean square error (RMSE) and R-squared [19] to validate the mapping effectiveness.

Algorithm 1 Reliability Mapping Through SVR&RF

Input: Reliability data x of all power converters, system reliability indicators y.
Output: Predicted system reliability indicators
Training:
1 Create a data set $\mathbf{X} = \{x_1, x_2, \ldots, x_n\}$ where each vector x_n denotes the No. n power converter reliability index at time t.
2 Create a data set Y for the system EENS and LOLE.
3 Apply ML regression algorithms:
$\hat{f}_{SVR} = \text{SVR}()$
$\hat{f}_{RF} = \text{RandomForestRegression}\ ()$
4 Train the and Y pairs to SVR and RF model. The ratio of training to testingdata is set as 8:2.
Testing:
5 Apply both trained models to the remaining data and calculate the predicted output $\hat{y}$.
6 Calculate RMSE and R-squared values to evaluate both mapping models.

IV. VARIANCE-BASED GLOBAL SENSITIVITY ANALYSIS

Since various uncertain parameters are involved in the nonlinear reliability relationship built in the first stage, an appropriate SA is essential to interpret the system behavior based on the information revealed by this relationship. More uncertainty parameters will be involved due to the proliferation of RESs and power electronic converters. However, it is computationally expensive, and it may not be necessary to monitor all uncertainties. Hence, identifying the most critical uncertainties, i.e., the most influential pair of an RES and its connected power converter on the system reliability will help system operators and stakeholders to better arrange the maintenance schedule and facilitate better system operation. Variance is a universal index to depict the output variability without hypothesis on the linearity or monotonicity of the model [15]. Therefore, in this stage, we apply the variance-based GSA to the proposed power system.

The variance-based GSA investigates the contribution of each uncertain input, to the selected output variance, either a single input variable, or multiple input combinations. This method has been applied to a variety of problems in the power system field, such as generators/loads ranking and distributed generation allocation. However, there are few papers that take power converter uncertainties into consideration when applying variance-based GSA. It is necessary to conduct an importance ranking from the power converter perspective, to improve the understanding of the power system reliability, and further provide useful advice for the system operator.

The theoretical background of the variance-based GSA algorithm is first introduced. The detailed specifications such as the input uncertainties and sensitivity indices are also defined.

A. THEORETICAL BACKGROUND

From a black box perspective, any model can be described by equation (14), where $\boldsymbol{X} = \{X_1, X_2, \ldots, X_n\}$ is a vector of n uncertain inputs, and Y is a selected univariate output.

$$Y = g(X_1, X_2, \ldots, X_n) \tag{14}$$

$$Var(Y) = \sum_{i=1}^{n} V_i + \sum_{1 \le i < j}^{n} V_{i,j} + \ldots + V_{1,2,\ldots,n} \tag{15}$$

Each input X_i follows a specific probability density function (PDF) and the variance $Var(Y)$ of Y can be decomposed as in equation (15) where V_i is the variance of Y caused by X_i without considering its interaction with other uncertain inputs, and $V_{1,2,\ldots,n}$ represents the proportion of $Var(Y)$ caused by $\{X_1, X_2, \ldots, X_n\}$.

From a power electronic converter perspective, the operating condition of a power converter can be described from the following parameters [7]: peak current, switching frequency, mean junction temperature, etc. In stage I, we can conclude that the converter voltage/current can be calculated from environmental data, and the junction temperature can be obtained from equation (X) given the ambient temperature value. Thus, regarding a WT converter i, the input uncertainties consist of wind speed v and temperature T, i.e., $X_i = \{v_i, T_i\}$. The solar irradiance S and temperature T represents the uncertainties in a PV converter j ($X_j = \{SR_j, T_j\}$). The switching frequency of

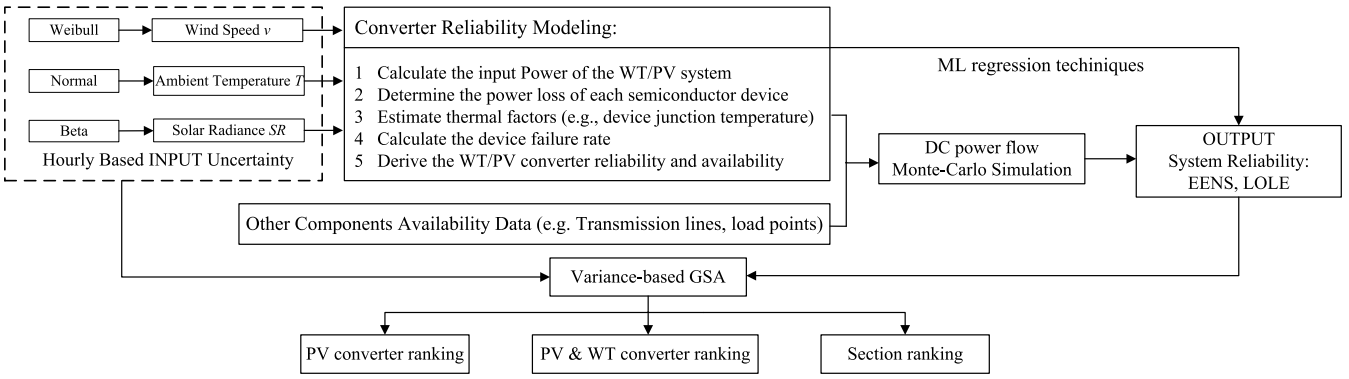

FIGURE 2. **An overview of the proposed reliability assessment on the power system.**

a power converter is assumed stable and not considered as an uncertainty.

The traditional reliability index *EENS* is used as the system output in the first stage, and its variance can be easily obtained. Thus, the variance of *EENS* is selected as the output $Var(Y)$ in the second stage.

B. SENSITIVITY INDICES

As described in equation (16), we have the Sobol' indices [21] defined in equation (16),

$$S_i = \frac{V_i}{Var(Y)}, \quad S_{ij} = \frac{V_{i,j}}{Var(Y)}, \; S_{1\ldots k} = \frac{V_{1,2\ldots,k}}{Var(Y)} \tag{16}$$

where S_i is the first-order index, $S_{i,j}$ is the second-order index, and $S_{1,2,\ldots,k}$ is the higher-order index corresponding to $\{X_1, X_2, \ldots, X_k\}$. Interactions of this kind will continue up to *nth* order for n uncertainties.

Thus, the number of indices and computational cost will increase dramatically if calculating the higher-order index. As a result, the first-order and total-effect Sobol' indices are commonly used.

1) First-order index—S_i: According to equation (16), the first-order index describes the contribution to the output variance of the effect from X_i, i.e., the effect of a single converter uncertainty to the system variance of *EENS*. Equation (17) is used to calculate each S_i [21]:

$$S_i = 1 - \frac{E\left[V\left(Y \mid X_i\right)\right]}{Var\left(Y\right)}, \quad S_i \in [0, 1] \tag{17}$$

where $E[V(Y|X_i)]$ denotes the expectation of the conditional variance of Y given X_i has a fixed value. This conditional expected variance is taken over all $X_j, j \neq i$, weighted by the density of X_i.

2) Total effect index—TE_i: As described in equation (16), there exist interaction terms such as $V_{i,j}$ and higher-order variance that represent the combined effect of multiple inputs. For a system with independent inputs, the total output variance can be described in (5):

$$\sum_i S_i + \sum_i \sum_{i<j} S_{i,j} + \sum_i \sum_{i<j} \sum_{j<k} S_{ijk} + \ldots = 1 \tag{18}$$

where S_i is the first-order index. $S_{i,j}$ is the second-order interaction index related to input i and j. Similarly, $S_{i,j,k}$ is the third-order interaction index.

The total effect index TE_i is defined as the sum of all terms in (18) that contain the subscript i, which describes the percentage of variance that remains if all inputs except X_i are specified and only X_i is a random variable. Thus, the total effect index can be calculated by equation (6):

$$TE_i = \frac{E[V(Y|X_{-i})]}{Var(Y)} \tag{19}$$

in which X_{-i} represents the vector of all X_j where $j \neq i$ (i.e., all parameters except X_i).

V. NON-SEQUENTIAL SAMPLING AND SYSTEM OVERVIEW

As shown in Fig. 2, we illustrate a system overview for the proposed framework. First, wind speed, ambient temperature and solar radiance, are considered as input uncertainties. These input data are collected under each hour to derive the WT/PV output power. Then, the reliability formulation introduced in Section II is adopted for each power converter. Reliability data of other system components, such as the failure rate of the transmission lines, diesel generators, load points, and station transformers, are also considered such that all component states can be determined. The system reliability indicators such as EENS and LOLE (and their variance), are calculated by conducting a DC power flow and the abovementioned non-sequential Monte Carlo method. The reliability relation between the converter and system stages is then established through SVR and RF algorithms. Finally, both the input uncertainties and the system EENS variance are selected to conduct the variance-based GSA. Sensitivity indices are generated to provide an importance ranking of the power converters.

We realize the system reliability calculation through a non-sequential Monte Carlo (MC) sampling approach for the following reasons. First, it requires less computational cost and memory compared to sequential MC method [22]. Second, non-sequential MC is a well-established method such that

easy implementation can be realized. The state of overall system is determined after finishing the probability sampling of all system components' states under each hour. We assume that there are multiple operating states on each WT/PV generator which is dependent on the level of its power output. Other components are assumed with two operating states: up and down. The probability of each state is calculated accordingly in (20) and (21), where $\lambda_{i,t}$ represents the failure rate of device i at hour t. The device repair rate μ_i is considered stable and assumed time-invariant.

$$\mathbb{P}_U(i,t) = \frac{\mu_i}{\lambda_{i,t} + \mu_i} \tag{20}$$

$$\mathbb{P}_D(i,t) = \frac{\lambda_{i,t}}{\lambda_{i,t} + \mu_i} \tag{21}$$

Then, we adopt a DC load flow based linear programming for each hour to calculate the power flow of each transmission line. The sampling process is repeated for a pre-determined number of iterations until the stopping criteria or limited calculation error is triggered. Eventually, both the input data and the calculated system EENS and LOLE values are collected for ML reliability mapping formulation introduced in Section III. The definition of EENS and LOLE are listed in Appendix D.

VI. NUMERICAL ANALYSIS

In this section, the proposed two-stage framework is validated on the modified 24-bus IEEE reliability test system (RTS). The computations, including non-sequential MC simulations, are performed in Matlab 2020a on an Intel Core at 2.90GHz with 16 GB RAM. ML regression models are implemented through Python sckit-learn. The software called SIMLAB [23] is adopted for the GSA calculations.

A. THE MODIFIED 24-BUS IEEE RTS

Fig.3 presents the modified 24-bus IEEE RTS network. We apply the latest version of RTS including the generation and load data [24]. Three WT and six PV generators and connected power converters have been added to the system. They are located at different buses with different capacities. The detailed information is in Appendix E.

B. THE REGRESSION MAPPING BETWEEN TWO STAGES

As introduced in Section III, both SVR and RF are integrated to investigate the nonlinear relation between converter and system stage reliability. We apply 80% of the converter/system reliability data as the training set, as well as determine the intrinsic parameters of both algorithms, while the remaining 20% is adopted for testing and further analysis. The computational cost of SVR and RF are 41.34s and 47.92s, respectively.

The RMSE derived from the SVR method is 1.943, which is lower than the value calculated by the RF method (2.221), while the R-squared value under SVR has a higher value which reaches 0.947 (0.921 under RF). Both R-squared values are above 0.9 which indicates that the predicted and actual

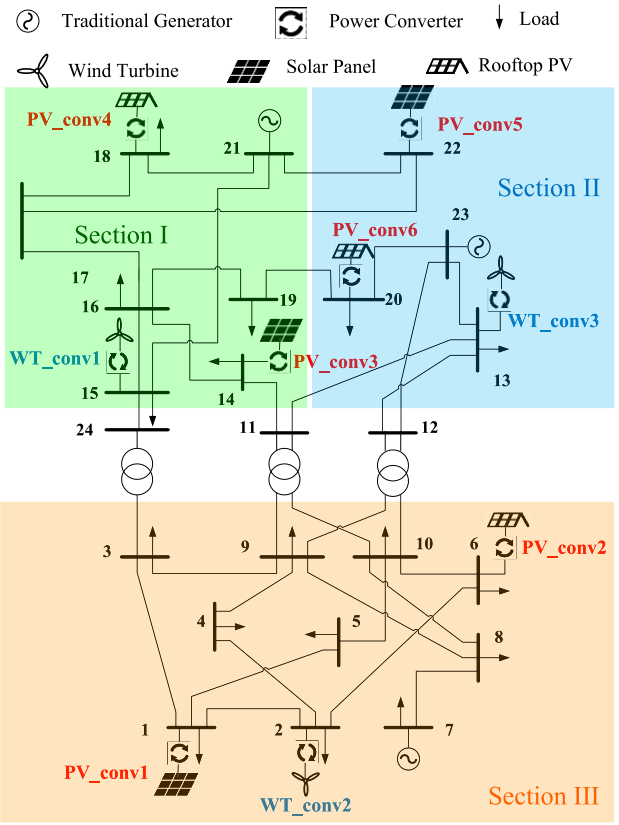

FIGURE 3. **The modified 24-bus IEEE RTS with RES and power converter penetration.**

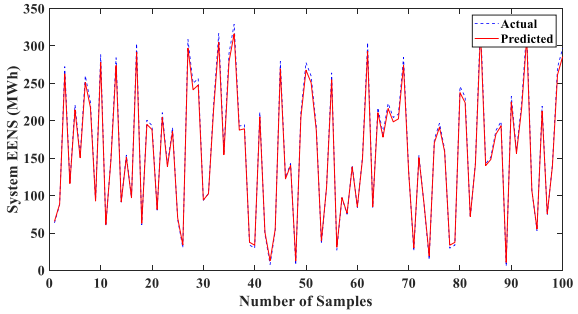

FIGURE 4. **Comparison between the predicted and actual EENS.**

system EENS values are basically matched with very limited error. As shown in Fig.4, 100 samples from testing set are illustrated to make comparisons between predicted EENS and corresponding actual values. In general, the predicted and actual EENS follow a similar pattern over all samples, and the maximum EENS difference reaches only 1.2%. The mapping results indicate that a reliability mapping between converter and system stages is applicable through ML algorithms.

C. VARIANCE-BASED GSA RESULTS AND MAINTENANCE SUGGESTIONS

To thoroughly conduct an importance ranking for converter uncertainties on the proposed power network, three cases are considered when implementing variance-based GSA:

TABLE 1. Sensitivity indices of PV converters under different sample sizes (e.g., $S_{PV_{conv1}} = 0.103_{(3)}$ indicates the first-order index is 0.103 and this PV converter is ranked No.3 among all PV converters).

No. of Samples	First-order indices $[S_{PV_{conv1}}, S_{PV_{conv2}}, \ldots, S_{PV_{conv6}}]$	Total-effect indices $[TE_{PV_{conv1}}, TE_{PV_{conv2}}, \ldots, TE_{PV_{conv6}}]$
50	$[0.103_{(3)}, 0.079_{(6)}, 0.119_{(1)}, 0.094_{(4)}, 0.113_{(2)}, 0.091_{(5)}]$	$[0.456_{(3)}, 0.313_{(6)}, 0.477_{(1)}, 0.382_{(4)}, 0.468_{(2)}, 0.341_{(5)}]$
100	$[0.102_{(3)}, 0.082_{(6)}, 0.114_{(1)}, 0.092_{(5)}, 0.113_{(2)}, 0.093_{(4)}]$	$[0.452_{(3)}, 0.314_{(6)}, 0.480_{(1)}, 0.391_{(4)}, 0.462_{(2)}, 0.342_{(5)}]$
500	$[0.105_{(3)}, 0.086_{(6)}, 0.124_{(1)}, 0.100_{(4)}, 0.111_{(2)}, 0.093_{(5)}]$	$[0.448_{(3)}, 0.308_{(6)}, 0.478_{(1)}, 0.390_{(4)}, 0.464_{(2)}, 0.340_{(5)}]$
1000	$[0.107_{(3)}, 0.084_{(6)}, 0.127_{(1)}, 0.098_{(4)}, 0.114_{(2)}, 0.095_{(5)}]$	$[0.449_{(3)}, 0.311_{(6)}, 0.481_{(1)}, 0.398_{(4)}, 0.462_{(2)}, 0.341_{(5)}]$
2000	$[0.110_{(3)}, 0.083_{(6)}, 0.128_{(1)}, 0.097_{(4)}, 0.112_{(2)}, 0.094_{(5)}]$	$[0.449_{(3)}, 0.312_{(6)}, 0.480_{(1)}, 0.394_{(4)}, 0.462_{(2)}, 0.343_{(5)}]$

Case Study 1. To focus on the analysis of each type of power converter, we consider the uncertainties of all six PVs and their converters which are marked as "PV_conv" in Fig.3.

Case Study 2. We consider new uncertainties from three WT systems ("WT_conv" in Fig.3) such that all converter uncertainties are considered in this case.

Case Study 3. The network is divided into three sections as shown in Fig.3, where each area includes both WT and PV converters. Moreover, we consider the load perturbation on each bus, e.g., between 2% and 5% [25]. The uncertainties in each section are grouped together to investigate their importance.

The analyzed results, i.e., the importance ranking under all three cases, can provide system reliability evaluation from the converter perspective so that system operators or stakeholders can identify the most uncertain/vulnerable converter or area and make proactive decisions.

1) CASE STUDY 1

In the first case, utility solar panels and rooftop PV systems are considered. The solar radiance *SR* and temperature *T* are used to represent the PV converter uncertainties. Beta and normal distributions are adopted for solar radiance and ambient temperature through $[a, b]$ and $[\mu, \sigma]$, respectively [25]. The probability distributions and probabilistic parameters of input uncertainties are presented in Appendix E.

Table 1 presents the $S1$ and TE values of all six PV converter uncertainties under different numbers of samples. The subscripts with parentheses indicate the rank of each PV converter. Both $S1$ and TE values provide almost identical results that the uncertainties of "PV_conv3" located at bus 14 have the largest values, i.e., 0.128 and 0.481, respectively, which indicates that the uncertainty of this converter contributes more system EENS variance compared to other converters. In other words, this converter is of the most important among all PV converters. From the results of TE, "PV_conv1", "PV_conv3" and "PV_conv5" have higher values, which means the system EENS variance value changed more when considering the uncertainty of these three PV converters compared to considering other converters. Thus, they are considered more important compared with the remaining three converters, in terms of the effect on system EENS variation. This is consistent with the fact that rooftop PVs such as "PV_conv6" has a smaller capacity and its failure results in less EENS compared with other utility PVs.

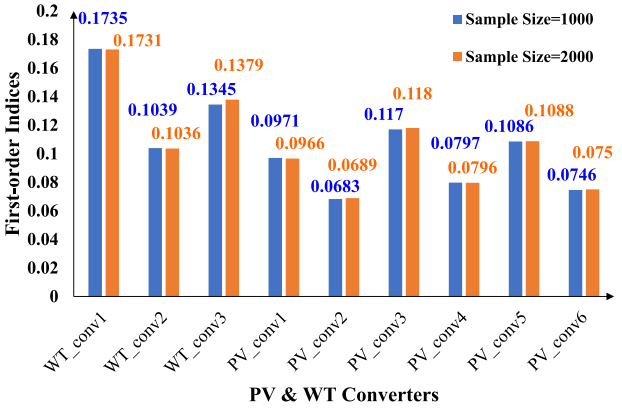

FIGURE 5. First-order indices of PV/WT converter uncertainties.

From the system reliability point of view, it can be concluded that the utility PV converters at buses 13, 22, and 1 are more important compared with the remaining three rooftop PV systems.

2) CASE STUDY 2

Based on case study 1, we add the uncertainties of all three WT systems in the second case. As described in Section IV, the wind speed v and temperature T are modeled as WT converter uncertainties. Weibull and normal distributions are adopted for wind speed and ambient temperature through $[\alpha, \beta]$ and $[\mu, \sigma]$, respectively [25].

As shown in Fig. 5 and Fig. 6, the sensitivity indices such as first-order $S1$ and total-effect index TE are calculated for all converter uncertainties under 1000 and 2000 sample size. The $S1$ and TE indices provide identical results that WT converter 1 located at bus 15 has the largest $S1$ (0.173) and TE (0.380) values among all the converters, which indicates

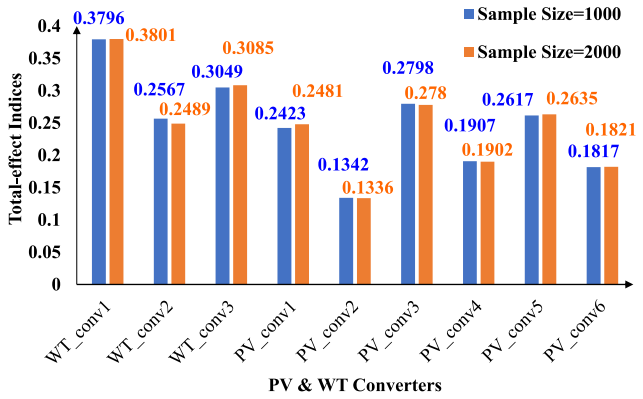

FIGURE 6. **Total-effect indices of PV/WT converter uncertainties.**

"WT_conv1" is the most important among all converters. "WT_conv3" located at bus 13 and "PV_conv3" at bus 14 are ranked at 2nd and 3rd place, respectively.

To explain the simulation results from the system network perspective, the "WT_conv1" has the largest capacity, while the "PV_conv2" has the lowest. Further, the WT generation on bus 15 normally will deliver power to several loads on different buses, such as bus 14, 16 and 18, while the "PV_conv2" supplies only a small load on bus 6. Thus, the system EENS does not vary much if a generation fluctuation occurs on "PV_conv2" or a failure happened on this converter.

As a conclusion, the converter uncertainty of "WT_conv1" is ranked as the most important affecting the system EENS variance, and the system operator should pay more attention to the WT system located at bus 15.

3) CASE STUDY 3

The system EENS may vary significantly due to a group of uncertainties in a specific geographical area. With increasing converters and loads integrated into the power system, it is desirable to conduct variance-based GSA on different areas, in which multiple converters' uncertainties and load perturbations are considered. In this case, the system network is divided into three sections, I, II and III, as shown in Fig. 3. Each section contains WT, and PV converters and several loads. Moreover, we introduce a 3% load perturbation on each bus. The load fluctuation parameters are listed in Appendix E. All uncertainties in each section, hence, are grouped together for consideration in this case. Since the first-order and total-effect indices provided almost identical results in previous cases, only the total-effect index is used in this case to save computational cost. This case is intended to highlight which area should receive more attention, and where the maintenance should be primarily scheduled.

Table 2 lists the distribution of all buses in each section, and Table 3 presents the total-effect index under different sampling sizes. Each subscript indicates the section ranking. All *TE* values are stable and the *TE* value on section I is the highest among all three sections under different sample sizes since both "WT_conv1" and "PV_conv3" are located within section I and are top-ranked based on the results from the previous two cases, which significantly increases the importance of this section. Section III contains more buses compared to the other two sections. However, it has the lowest *TE* value. The average load demand in I is the highest while section III has the smallest load requirement. Thus, intuitively, the system EENS variance is more sensitive to section I.

TABLE 2. **Bus information of each section.**

	Involved Buses
Section I	14, 15, 16, 17, 18, 19, 21
Section II	13, 20, 22, 23
Section III	1, 2, 3, 4, 5, 6, 7, 8, 9, 10

TABLE 3. **Total-effect indices for each divided area.**

No. of Samples	Sections I	II	III
50	$1.271_{(1)}$	$1.065_{(2)}$	$0.874_{(3)}$
100	$1.276_{(1)}$	$1.041_{(2)}$	$0.865_{(3)}$
500	$1.272_{(1)}$	$1.040_{(2)}$	$0.853_{(3)}$
1000	$1.296_{(1)}$	$1.057_{(2)}$	$0.870_{(3)}$
2000	$1.289_{(1)}$	$1.053_{(2)}$	$0.860_{(3)}$

Since resources are limited, maintenance efforts should be optimally distributed into multiple sections. Thus, the results from this area-based analysis provide a more comprehensive importance ranking which can help the system operator understand the ultimate effect on system reliability resulting from the uncertainties of a geographical area. This case evaluates the converter uncertainty and load fluctuation of each section and thus, is critical for system operators in scheduling better maintenance and mitigating potential failure risk.

VII. CONCLUSION AND FUTURE WORKS

This paper proposes a two-stage reliability framework for a power system. In the first stage, we formulate the reliability of each converter while considering critical semi-conductor devices. The system reliability indicators are calculated through a non-sequential MC approach. Afterward, a nonlinear relationship is established through ML regression techniques. A variance-based GSA is applied in the second stage to conduct an importance ranking for different groups of power converters. The numerical results validate the premise that uncertainties introduced by RESs and converters have a non-negligible impact on the overall power system reliability. Future works will focus on exploring the repair strategy for critical devices and converters, and its reliability impact on power system network variations (i.e., different network topologies). Moreover, we will explore the optimization of reliability cost for a converter-dominated system, the impact of the battery capacity, the storage location, and the implementation of ML interpreting approaches to enhance the explanation of the reliability and provide comprehensive information for system operators.

ACKNOWLEDGMENT

The authors would like to thank the anonymous editor and reviewers for their valuable comments and suggestions to improve the quality of this paper.

REFERENCES

[1] S. Peyghami, F. Blaabjerg, and P. Palensky, "Incorporating power electronic converters reliability into modern power system reliability analysis," *IEEE J. Emerg. Sel. Topics Power Electron.*, vol. 9, no. 2, pp. 1668–1681, Apr. 2021.

[2] K. Hou, H. Jia, X. Xu, Z. Liu, and Y. Jiang, "A continuous time Markov chain based sequential analytical approach for composite power system reliability assessment," *IEEE Trans. Power Syst.*, vol. 31, no. 1, pp. 738–748, Jan. 2016.

[3] N. Nguyen and J. Mitra, "Reliability of power system with high wind penetration under frequency stability constraint," *IEEE Trans. Power Syst.*, vol. 33, no. 1, pp. 985–994, Jan. 2018.

[4] P. Zhang, Y. Wang, W. Xiao, and W. Li, "Reliability evaluation of grid-connected photovoltaic power systems," *IEEE Trans. Sustain. Energy*, vol. 3, no. 3, pp. 379–389, Jul. 2012.

[5] Y. Ding, C. Singh, L. Goel, J. Østergaard, and P. Wang, "Short-term and medium-term reliability evaluation for power systems with high penetration of wind power," *IEEE Trans. Sustain. Energy*, vol. 5, no. 3, pp. 896–906, Jul. 2014.

[6] A. Ahadi, N. Ghadimi, and D. Mirabbasi, "Reliability assessment for components of large scale photovoltaic systems," *J. Power Sources*, vol. 264, pp. 211–219, Oct. 2014.

[7] S. Yang, A. Bryant, P. Mawby, D. Xiang, L. Ran, and P. Tavner, "An industry-based survey of reliability in power electronic converters," *IEEE Trans. Ind. Appl.*, vol. 47, no. 3, pp. 1441–1451, May 2011.

[8] G. Adinolfi, G. Graditi, P. Siano, and A. Piccolo, "Multiobjective optimal design of photovoltaic synchronous boost converters assessing efficiency, reliability, and cost savings," *IEEE Trans. Ind. Informat.*, vol. 11, no. 5, pp. 1038–1048, Oct. 2015.

[9] B. Zhang, M. Wang, and W. Su, "Reliability analysis of power systems integrated with high-penetration of power converters," *IEEE Trans. Power Syst.*, vol. 36, no. 3, pp. 1998–2009, May 2021.

[10] C. Peng, S. Lei, Y. Hou, and F. Wu, "Uncertainty management in power system operation," *CSEE J. Power Energy Syst.*, vol. 1, no. 1, pp. 28–35, Mar. 2015.

[11] K. N. Hasan, R. Preece, and J. V. Milanović, "Priority ranking of critical uncertainties affecting small-disturbance stability using sensitivity analysis techniques," *IEEE Trans. Power Syst.*, vol. 32, no. 4, pp. 2629–2639, Jul. 2017.

[12] R. Preece and J. V. Milanović, "Assessing the applicability of uncertainty importance measures for power system studies," *IEEE Trans. Power Syst.*, vol. 31, no. 3, pp. 2076–2084, May 2016.

[13] A. Gonzalez, F. M. Echavarren, L. Rouco, and T. Gomez, "A sensitivities computation method for reconfiguration of radial networks," *IEEE Trans. Power Syst.*, vol. 27, no. 3, pp. 1294–1301, Aug. 2012.

[14] F. Tamp and P. Ciufo, "A sensitivity analysis toolkit for the simplification of MV distribution network voltage management," *IEEE Trans. Smart Grid*, vol. 5, no. 2, pp. 559–568, Mar. 2014.

[15] V. Calderaro, G. Conio, V. Galdi, G. Massa, and A. Piccolo, "Optimal decentralized voltage control for distribution systems with inverter-based distributed generators," *IEEE Trans. Power Syst.*, vol. 29, no. 1, pp. 230–241, Jan. 2014.

[16] F. Ni, M. Nijhuis, P. H. Nguyen, and J. F. G. Cobben, "Variance-based global sensitivity analysis for power systems," *IEEE Trans. Power Syst.*, vol. 33, no. 2, pp. 1670–1682, Mar. 2018.

[17] S. E. De Leon-Aldaco, H. Calleja, and J. A. Alquicira, "Reliability and mission profiles of photovoltaic systems: A FIDES approach," *IEEE Trans. Power Electron.*, vol. 30, no. 5, pp. 2578–2586, May 2015.

[18] H. Liu *et al.*, "A nonlinear regression application via machine learning techniques for geomagnetic data reconstruction processing," *IEEE Trans. Geosci. Remote Sens.*, vol. 57, no. 1, pp. 128–140, Jan. 2019.

[19] N. Nava, T. Matteo, and T. Aste, "Financial time series forecasting using empirical mode decomposition and support vector regression," *Risks*, vol. 6, no. 1, p. 7, Feb. 2018.

[20] X. Wu, J. He, T. Yip, J. Lu, and N. Lu, "A two-stage random forest method for short-term load forecasting," in *Proc. IEEE Power Energy Soc. Gen. Meeting (PESGM)*, Jul. 2016, pp. 1–5.

[21] Z. Hu and S. Mahadevan, "Probability models for data-driven global sensitivity analysis," *Rel. Eng. Syst. Saf.*, vol. 187, pp. 40–57, Jul. 2019.

[22] H. Lei and C. Singh, "Non-sequential Monte Carlo simulation for cyber-induced dependent failures in composite power system reliability evaluation," *IEEE Trans. Power Syst.*, vol. 32, no. 2, pp. 1064–1072, Mar. 2017.

[23] N. Delgarm, B. Sajadi, K. Azarbad, and S. Delgarm, "Sensitivity analysis of building energy performance: A simulation-based approach using OFAT and variance-based sensitivity analysis methods," *J. Building Eng.*, vol. 15, pp. 181–193, Jan. 2018.

[24] C. Barrows *et al.*, "The IEEE reliability test system: A proposed 2019 update," *IEEE Trans. Power Syst.*, vol. 35, no. 1, pp. 119–127, Jan. 2020.

[25] L. Bilir, M. Imir, Y. Devrim, and A. Albostan, "Seasonal and yearly wind speed distribution and wind power density analysis based on weibull distribution function," *Int. J. Hydrogen Energy*, vol. 40, no. 44, pp. 15301–15310, Nov. 2015.

[26] K. Xie, Z. Jiang, and W. Li, "Effect of wind speed on wind turbine power converter reliability," *IEEE Trans. Energy Convers.*, vol. 27, no. 1, pp. 96–104, Mar. 2012.

[27] FIDES Guide. (Sep. 2010). *A Reliability Methodology for Electronic Systems*. [Online]. Available: https://www.fides-reliability.org

BOWEN ZHANG (Graduate Student Member, IEEE) received the B.S. degree in electrical engineering from Southeast University, Nanjing, China, in 2015, and the M.S. degree in electrical engineering from the University of Michigan-Dearborn, Dearborn, MI, USA, in 2017, where he is currently pursuing the Ph.D. degree in electrical engineering. His current research interests include power electronics, power system reliability, and machine learning.

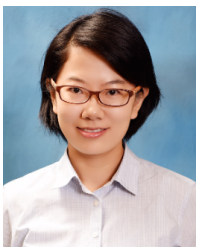

MENGQI WANG (Senior Member, IEEE) received the B.S. degree in electrical engineering from Xi'an Jiaotong University, Xi'an, in 2009, and the Ph.D. degree in electrical engineering from North Carolina State University, Raleigh, NC, USA, in 2014. She is currently an Associate Professor with the Department of Electrical and Computer Engineering, University of Michigan-Dearborn, USA. Her research interests include dc–dc and dc–ac power conversions, high-efficiency and high-power-density power supplies, renewable energy systems, and wide-bandgap power device applications.

WENCONG SU (Senior Member, IEEE) received the B.S. degree (Hons.) from Clarkson University, Potsdam, NY, USA, in 2008, the M.S. degree from Virginia Tech, Blacksburg, VA, USA, in 2009, and the Ph.D. degree from North Carolina State University, Raleigh, NC, USA, in 2013. He is currently an Associate Professor with the Department of Electrical and Computer Engineering, University of Michigan-Dearborn, USA. He has authored 1 book, 4 book chapters, and over 100 high-quality articles in prestigious international journals and peer-reviewed conference proceedings. His current research interests include power systems, electrified transportation systems, and cyber-physical systems. He is a Fellow of IET. He was a recipient of the 2015 IEEE Power and Energy Society (PES) Technical Committee Prize Paper Award and the 2013 IEEE Industrial Electronics Society (IES) Student Best Paper Award. He is an Editor of IEEE Transactions on Smart Grid, an Associate Editor of IEEE Access, and an Associate Editor of IEEE DataPort. He is an Editor of IEEE Transactions on Smart Grid, an Associate Editor of IEEE Access, and an Associate Editor of IEEE DataPort. He is the Guest Editor-in-Chief of IEEE Transactions on Smart Grid - Special Section on Power-Electronics-Enabled Smart Power Distribution Grid. He is a registered Professional Engineer (P.E.) in the State of Michigan, USA.